Author/s:
Harris, AR;Carter, P;Cowan, R;Wallace, GG

Title:
Impact of Protein Fouling on the Charge Injection Capacity, Impedance, and Effective Electrode Area of Platinum Electrodes for Bionic Devices

Date:
2021-03-12

Citation:
Harris, A. R., Carter, P., Cowan, R. & Wallace, G. G. (2021). Impact of Protein Fouling on the Charge Injection Capacity, Impedance, and Effective Electrode Area of Platinum Electrodes for Bionic Devices. Chemelectrochem, 8 (6), pp.1078-1090. https://doi.org/10.1002/celc.202001574.

Persistent Link:
https://hdl.handle.net/11343/274300

Title: The Impact of Protein Fouling on the Charge Injection Capacity, Impedance and Effective Electrode Area of Platinum Electrodes for Bionic Devices

Authors: Alex Harris; Paul Carter; Robert Cowan; Gordon G. Wallace

To be cited as: 10.1002/celc.202001574

Link to VoR: https://doi.org/10.1002/celc.202001574

The Impact of Protein Fouling on the Charge Injection Capacity, Impedance and Effective Electrode Area of Platinum Electrodes for Bionic Devices

Alexander R. Harris*[1,2], Paul Carter[3], Robert Cowan[2,4], Gordon G. Wallace[5]

[1] Aikenhead Centre for Medical Discovery, ARC Centre of Excellence for Electromaterials Science, Faculty of Medicine, Dentistry and Health Sciences, University of Melbourne, Melbourne, Vic, 3010, Australia

[2] The HEARing CRC, 550 Swanston St, University of Melbourne, Melbourne, 3010, Australia

[3] Cochlear Ltd, 1 University Ave, Macquarie University, NSW, 2109, Australia

[4] Department of Audiology & Speech Pathology, 550 Swanston St, University of Melbourne, Melbourne, 3010, Australia

[5] ARC Centre of Excellence for Electromaterials Science, Intelligent Polymer Research Institute, University of Wollongong, Wollongong, NSW, 2522, Australia

*Email: alexrharris@gmail.com

Abstract

The impact of protein fouling on platinum electrodes was assessed by electrochemical methods. Protein fouling affected the electrode potential and charge transfer through the electrode-solution interface. Adsorbed proteins partially blocked the electrode, with no charge passing through blocked regions. The electrochemical theory and methodology for investigating partially blocked electrodes is fully presented, applied to protein adsorption and the implications for bionics applications are discussed. The partially blocked electrode had a reduced admittance, and increased impedance and polarisation resistance consistent with a smaller effective electrode area. The charge storage capacity and charge injection capacity decreased after protein adsorption. The effective electrode area was assessed by impedance and cyclic voltammetry. The diffusion profile towards the partially blocked electrode was mixed between linear and radial diffusion.

Keywords

cochlear implant; impedance test; platinum; protein fouling

1. Introduction

Electrodes have been developed to interact with neural and muscle tissue to measure and control their electrophysiological activity. These electrodes are used for research into tissue function and treatment of various disorders.

The cochlear implant is able to provide auditory cues for people with profound sensorineural hearing loss [1]. Electrodes are placed into the fluid-filled cochlea within the temporal bone. Charge delivered from the electrodes induces activity in nearby auditory fibres, and ultimately elicits a sound percept in the brain.

In other work, electrodes placed onto or into the brain have been developed to detect epileptic seizures [2], control movement disorders such as Parkinson's disease [3] and provide sound percepts through auditory brainstem implants [4]. In addition, peripheral nerves have been targeted for electrical stimulation for the treatment of numerous intractable disorders including incontinence, chronic pain and vision loss [5][6][7].

In general, implantable electrodes are constructed from platinum or platinum-iridium, as these materials have been shown to be corrosion resistant, biocompatible and highly conductive. While the goal of implantable electrodes for stimulation is to induce activity in nearby cells, charge delivery requires transduction of electrical current in the electronics into ion migration within the tissue. This conversion is achieved through electrochemical reactions at the electrode-tissue interface. Ideally the reactions occurring at the electrode-tissue interface would be "innocent", by not affecting the electrode or surrounding tissue. However generation of cytotoxic species and electrode corrosion can occur, including reactions such as $\mathrm{Pt}+4\mathrm{Cl}^- \rightarrow [\mathrm{PtCl}_4]^{2-} + 2e^-$ [8]. These reactions can kill the target tissue and degrade the electrode, leading to device failure.

The performance of electrodes is typically assessed by a series of on the bench protocols [9]. Electrochemical methods are used to measure the amount of charge that can be supplied by the electrode, what reaction mechanisms occur at the electrode-solution interface and to determine the impedance characteristics. These in vitro tests are used to predict performance, biostability and formation of cytotoxic species generated at the electrode surface when it is implanted. However, these in vitro tests are generally performed over short time periods, whereas implanted electrodes are expected to function consistently in vivo for decades. The electrodes are also exposed to highly dynamic conditions with repeated high density current pulses applied in a complex biological milieu. Undetectable/low levels of corrosion or formation of cytotoxic species that occur in vitro may therefore build up over long term clinical use. It is therefore critical to understand how these devices function in clinically relevant conditions.

Early electrochemical studies on platinum electrodes applied short current pulses in simple electrolyte or acid solutions [10][11]. Platinum corrosion was then detected by spectrophotometric analyses of the electrolyte solution [12]. Variations in the applied waveform, including varying which of the cathodic or anodic pulses was first applied, affected the corrosion rate [13]. Follow up studies with the addition of protein to the test solution significantly reduced the corrosion rate [14]. But it was questioned whether the corrosion rate was physiologically relevant. Subsequent stimulation of platinum electrodes in a feline cortex was performed and corrosion products were detected [15][16].

Since these early studies, there have been significant advances in our understanding of the structure of platinum, tissue composition, electrochemical theory and techniques. This allows us to revisit the electrochemical behaviour of the electrode-tissue interface to gain a greater understanding of the charge transfer processes occurring there. We have recently investigated the impact of electrode structure, materials, solution composition and applied waveform at this interface [17][18][19][20][21][22]. This article now investigates the impact of proteins on charge transfer from the electrode.

Previous studies of protein exposure to electrode surfaces have been studied by numerous analytical techniques. Cyclic voltammetric measurements displayed a change in shape after protein adsorption, which was taken as a reduction in electron transfer rate [23][24]. However more fundamental electrochemical studies have shown an apparent decrease in rate constant can be caused by partial blocking of small domains on a larger electrode [25][26]. In order to distinguish the cause of the apparent decrease in rate constant, an in depth study of the impact of protein exposure on electrochemical behaviour must be undertaken. The voltammetric, chronopotentiometric and electrochemical impedance spectroscopic responses are characterised before and after exposure to individual and mixed proteins. The theory and methodology for measuring partially blocked electrodes is detailed and the effective electrode area is subsequently measured by impedance and voltammetric methods. Finally the impact of protein exposure to electrodes used in bionics applications is discussed.

2. Experimental Methods

Chemicals

Sodium chloride, potassium chloride, sodium bicarbonate, calcium chloride, D-glucose, hexaammineruthenium(III) chloride ($Ru(NH_3)_6Cl_3$), bovine serum albumin (BSA), fibrinogen from bovine plasma, soybean trypsin inhibitor, foetal bovine serum (FBS) (Sigma-Aldrich), magnesium chloride hexahydrate (Scharlau), monosodium phosphate (Biochemicals), 32 % hydrochloric acid (RCI Labscan) were used as received. An artificial perilymph (AP) contained 125 mM NaCl, 3.5 mM KCl, 25 mM $NaHCO_3$, 1.2 mM $MgCl_2$, 1.3 mM $CaCl_2$, 0.75 mM NaH_2PO_4 and 5 mM glucose [27]

and had a pH of 8.1. Where indicated, addition of HCl was used to lower the artificial perilymph pH to 5.5.

Electrode Preparation

A 0.6 mm diameter platinum disc (CH Instruments) was used as the working electrode. The electrode was freshly polished before every experiment with 0.3 μm alumina slurry on Microcloth polishing cloth (Buehler), rinsed in deionised water and gently dried (Kimwipe) before use. Protein adsorption was achieved by immersing the electrode in a 1 mg mL^{-1} solution of the protein in deionised water or in FBS for 10 minutes; the electrode was removed from the solution and excess solution wicked away with a Kimwipe. Electrodes were only used once before repolishing, to minimise any desorption of proteins into the test solution. The effective electrode area was measured with a 5.1 mM solution of $Ru(NH_3)_6Cl_3$ in artificial perilymph. A 3-electrode configuration was used with a Ag/AgCl (3 M KCl) as reference electrode and Pt wire as counter electrode on a CHI660E potentiostat (CH Instruments). The electrodes were connected to the potentiostat via alligator clips and placed into a beaker of solution. Test solutions were degassed with nitrogen for at least 10 minutes before use.

Applied Waveforms and Analysis

Cyclic voltammetry was performed with a potential window of 0.8 to -0.8 V at a scan rate of 100 mV s^{-1}. The charge storage capacity (CSC) was measured from the second cycle by transforming the current-potential plot to a current-time plot and integrating the reduction and oxidation sweeps separately. Cyclic voltammetry of $Ru(NH_3)_6Cl_3$ was performed over the potential range of 0 to -0.5 V with varying scan rate. The voltammetric response of $Ru(NH_3)_6Cl_3$ was fitted with DigiElch (Gamry). No background subtraction was performed on voltammetric responses.

Electrochemical impedance spectroscopy (EIS) was performed at 0 V with an AC amplitude of 5 mV over a frequency range of 0.1-100,000 Hz. Equivalent circuit fitting of the EIS data was performed with ZView (Scribner Associates).

Chronopotentiometic experiments were performed with a biphasic oxidation and reduction waveform of equal pulse length and magnitude but no interphase gap or interpulse interval. In each run, 4 biphasic pulses were applied. The charge density was 10 μC cm^{-2}, a value typical of that used in modern cochlear implants. The cochlear implant typically uses 25 μs current pulses, however the shortest pulse achievable on the commercial potentiostat was 5 ms. Therefore the applied charge (Q) was calculated by multiplying the charge density by the nominal electrode area (A); the current (i) for the 5 ms time pulse was then calculated from the total charge passed and the time (t), $i = Q / t$; (5.65 μA on a 600 μm diameter electrode resulting in 28.3 nC $phase^{-1}$). This charge density and charge per phase is considered safe according to the Shannon plot [28]. By definition, the larger the change in

potential measured during the chronopotentiometric pulse, the smaller is the electrode's charge injection capacity. To eliminate variability from the open circuit potential, the change in potential during the second pulse was measured (Figure 2a). The stability of the electrode to multiple pulsing was assessed by measuring the change in potential from the end of the second pulse to the end of the last pulse (cumulative 6 pulses).

3. Results

Open-Circuit Potential and Cyclic Voltammetry of Platinum Before and After Exposure to Protein Solutions

The open-circuit potential (OCP) of an unmodified, mechanically polished platinum electrode in artificial perilymph was 146 mV (Table 1). The cyclic voltammetry results were very similar to previous reports (Figure 1) [17] wherein a current peak at -63 mV due to platinum oxide reduction and further current below ~-460 mV due to hydrogen adsorption are observed. On the oxidation sweep, hydrogen desorption current extends to ~-350 mV and platinum oxide formation begins at ~110 mV. The CSC of the reduction and oxidation sweeps was again similar to previous measurements at 5.3 and 4.5 μC respectively (Table 1) [17].

A freshly polished electrode was placed into a protein solution, 1 mg mL^{-1} in deionised water for 10 minutes. This protein concentration is similar to that found in human perilymph [29]. Previous atomic force microscopy and ellipsometry measurements of platinum in contact with protein containing solutions displayed an increase in adsorbed layer thickness and roughness over time [30]. And quartz crystal microbalance studies of platinum placed in contact with protein containing solutions have shown a mass increase on the electrode, consistent with protein adsorption [31]. It was found that exposure of platinum to protein containing solutions for 10 minutes induced reproducible, steady-state mass adsorption. BSA, fibrinogen and trypsin inhibitor were chosen as low cost, readily available proteins that represent 3 of the highest concentration protein classes (albumins, glycoproteins and protease inhibitors) in perilymph [32]. They also have a range of molecular weights, sizes and isoelectric points to assess their impact on electrochemical behaviour (BSA 66 kDa, isoelectric point 4.7; fibrinogen 340 kDa, isoelectric point 5.5; soybean trypsin inhibitor 20 kDa, isoelectric point 9-10) [33].

The OCP of the electrodes exposed to different proteins was 70-85 mV more positive than the uncoated electrode (Table 1). BSA with the most negative charge had the greatest positive shift in OCP. The cyclic voltammetry obtained was similar to the unmodified electrode, with the platinum oxide reduction peak shifting to -88 mV, -95 mV and -96 mV after exposure to BSA, fibrinogen and trypsin inhibitor respectively (Figure 1). The current magnitude attributed to the hydrogen adsorption and desorption processes was smaller after exposure to proteins. The CSCc after BSA and fibrinogen

exposure was within error of the unmodified platinum electrode, but after exposure to trypsin inhibitor CSCc and all CSCa were significantly diminished (Table 1).

FBS was tested as a more complex protein solution that is often used to model *in vivo* environments. The OCP of a platinum electrode exposed to FBS was 30 mV more negative than the pristine electrode (Table 1). The platinum oxide reduction peak shifted from -63 mV to -93 mV; the current magnitude of the hydrogen adsorption and desorption process was lower but the oxidation current in the oxide formation region was slightly larger than the unmodified platinum, which may be due to amino acid adsorption (Figure 1) [34]. The CSCc electrode exposed to FBS was smaller than the unmodified electrode, but the CSCa was unchanged (Table 1).

Chronopotentiometry of Platinum Before and After Exposure to Protein Solutions

The charge injection capacity is measured from the change in electrode potential when a current pulse is applied. The charge injection capacity is related to CSC, with larger CSC generally resulting in a larger charge injection capacity (smaller change in potential during a current pulse) [19]. A cathodic pulse drives the electrode to negative potentials, while an anodic pulse leads to more positive potentials (Figure 2). The electrode potential is initially at OCP, so that an initial cathodic pulse polarity results in lower potentials than an initial positive polarity. For a pristine platinum electrode, the change in electrode potential was ~220-240 mV with either an anodic or cathodic first pulse polarity, in agreement with previous measurements (Table 2) [19]. Following multiple pulses, the electrode potential shifts (ratchets) more positively after an initial cathodic pulse; and more negatively with an initial anodic pulse [35]. A shift of ~25 mV was observed after 6 consecutive pulses.

The change in potential observed for platinum exposed to a BSA containing solution was slightly larger than that observed for pristine platinum, however after exposure to fibrinogen or trypsin inhibitor a change in potential of ~100 mV was observed (Table 2). The cumulative change in potential was also similar between the BSA and pristine platinum while fibrinogen and trypsin inhibitor exposure was ~5 mV larger. These trends are not perfectly correlated with the CSC values.

The FBS modified electrode had a change in potential that was 140-160 mV larger than the unmodified electrode. The cumulative change was 15-20 mV greater too. This change is in contrast to the very similar CSC between the unmodified platinum and FBS.

Electrochemical Impedance Spectroscopy of Platinum Before and After Exposure to Protein Solutions

The impedance of a platinum electrode in artificial perilymph had an increase in total impedance with decreasing frequency (Figure 3a). The phase angle was near 0 degrees at high frequency, with a peak

at -75 degrees at 17 Hz (Figure 3b). The Nyquist plot had a slight curvature (Figure 3c) in agreement with previous reports [20]. While the impedance at 1 kHz is often quoted for electrodes used in bionics applications, the utility of this measurement is limited, rather the impedance at low frequencies is more dependent on electrode properties and a better predictor of thermal noise and signal to noise ratio of electrophysiological recordings [22]. The impedance at 12 Hz is listed in Table 3 for reference.

An equivalent electrical circuit comprising a resistor (R1) in series with a parallel resistor (R2) and constant phase element (CPE1), which has been used previously for protein adsorption on platinum (Figure 3) [36], was applied to the impedance data. R1 represents the solution resistance, while the electrode-solution interface is modelled by a polarisation resistance (R2), and CPE1. The use of a constant phase element rather than a capacitor is thought to be due to inhomogeneous current distribution over the electrode surface or surface roughness [37]. Fitted parameters for the equivalent circuit are resistance, and admittance (Q_0) and power (n) terms for the constant phase element, which are again in close agreement with previous measurements (Table 3) [20].

Following exposure to BSA, fibrinogen, trypsin inhibitor or FBS, a similar impedance response was obtained (Figure 3). The impedance at low frequencies increased compared to the uncoated electrode in the order BSA = fibrinogen < trypsin inhibitor < FBS (Table 3). There were shifts in the phase angle with a more capacitive behaviour at high frequencies and more resistive at intermediate frequencies. The same equivalent circuit was fit to all systems. There were small variations in the solution resistance. Much larger changes could be seen with increased polarisation resistance and decreasing admittance, consistent with the increasing total impedance trend at low frequencies. These trends are all indicative of a decrease in effective electrode area, which increases low frequency impedance and polarisation resistance and decreases admittance [20][38]. Previous measurements have also shown an increase in polarisation resistance and decrease in admittance with adsorption of ploy-L-lysine or laminin onto a platinum electrode [36].

Electrode capacitance (C) is related to effective electrode area (A)

$$C = \varepsilon \varepsilon_0 A / d \tag{1}$$

where ε is the solution dielectric constant, ε_0 is the permittivity of free space and d is the double layer thickness. The impedance of a constant phase element is given by

$$Z = 1/[Q_0 (j * w)^n] \tag{2}$$

Capacitance is not equivalent to Q_0, so calculation of electrode area directly from Q_0 by substitution into equation 1 is not valid. The capacitance can be calculated from an equivalent circuit with a parallel CPE and resistor

$$C_{\omega_{\mathrm{m}}^{''}} = Q_0(\omega_{\mathrm{m}}^{''})^{\mathrm{n}-1} \quad (3)$$

where $\omega_{\mathrm{m}}^{''}$ is the frequency at which the imaginary impedance (Z'') is a maximum [39]. This frequency is at the top of a depressed semicircle on the Nyquist plot. The plots obtained here do not show the entire semicircle, and taking the maximum Z'' at 0.1 Hz would not give the true electrode capacitance or provide useful comparisons between measurements. It was not possible to apply smaller frequencies due to background noise and solution convection affecting the response. Alternatively, the capacitance can be calculated from

$$(C * R)^n = Q_0 * R \quad (4)$$

$$C = (Q_0 * R)^{(1/n)} / R \quad (5)$$

where R is the polarisation resistance, and is the width of the semicircle as it crosses the x axis of the Nyquist plot. While the semicircle is not fully formed here, simulations can provide R and allow comparison of experiments. The fraction of electrode which was blocked by protein adsorption fraction (θ) was determined from the relative values of capacitance and ranged up to 0.2 for individual proteins and 0.5 for FBS. However the accuracy of the simulation decreases and standard deviation increases with increasing R. Further assumptions are required that any changes in Q_0 are only due to variations in electrode area, and that changes to surface roughness, chemical functionality (amount of oxide, anion adsorption etc) and time constants from protein adsorption are negligible. Equations 3-5 are only valid for a parallel CPE and resistor, they are not valid for other equivalent circuits. These equations also assume the electrode is an ideal capacitor; however the true electrode capacitance typically varies with potential and applied frequency. Previous estimates of θ were made from a capacitance measurement of BSA adsorption onto a platinum electrode [40]. The capacitance decreased after protein adsorption, but the authors noted that the model was not valid, suggesting a negative protein layer thickness.

Effect of pH on Electrochemical Response of Platinum Before and After Exposure to Protein Solutions

Proteins contain charged residues that are pH dependant, resulting in a non-charged isolelectric point. In the electrochemical experiments reported above, BSA and fibrinogen would have had a net negative charge, while trypsin inhibitor would have had a net positive charge. To determine the impact of protein charge on the electrochemical response of a modified electrode, the pH of the artificial perilymph was lowered to 5.5, the isoelectric point of fibrinogen. Fibrinogen was adsorbed onto the electrode from the same 1 mg mL^{-1} in deionised water to eliminate any effects of protein concentration or amount of protein adsorption.

The electrochemical response of platinum is pH dependant, therefore the response of the unmodified electrode was initially tested in the pH 5.5 artificial perilymph (Figure 4). Compared to pH 8.2, the OCP was slightly negatively shifted by 12 mV (Table 1). A similar shaped response was seen to pH 8.2, with the current peak for platinum oxide reduction occurring at -58 mV compared to -63 mV for the pristine electrode, and the current associated with hydrogen adsorption and desorption being smaller (Figure 4). As a result, the anodic and cathodic CSC was smaller at pH 5.5.

When the electrode was coated with fibrinogen, the OCP was 83 mV more positive than the uncoated platinum (Table 1). This shift in potential is similar as occurred at pH 8.2. The voltammetry was again similar in shape, with the peak for the platinum oxide reduction appearing at -111 mV, 16 mV more negative than at pH 8.2 (Figure 4). The cathodic CSC was slightly increased and the anodic CSC decreased compared to the uncoated electrode, however both were significantly smaller than at pH 8.2.

The chronopotentiometric response appeared similar at the different pH (Figure 5). The change in potential after the second pulse and cumulative 6 pulses was in the same region (Table 2).

The impedance at pH 5.5 had the same profile as at pH 8.2 and was fit with the same equivalent circuit (Figure S1). While the polarisation resistance of unmodified platinum was larger at pH 5.5, all other fitted parameters and the impedance at 12 Hz were unaffected by the change in pH (Table 3).

In general, the impact of changing the pH affected the OCP of the electrode, shifting the voltammetric response to more negative potentials. This reduced the contribution of hydrogen adsorption and desorption to the CSC measured over a fixed potential range of 0.8 to -0.8 V. However the charge injection capacity and impedance response was largely unaffected.

Electrochemical Response of Platinum in Serum

In the above experiments, protein exposure was confined to the working electrode surface. However, in the body, proteins will also be present in the solution between the electrodes and in contact with the reference electrode. To assess these conditions, the electrode was first coated with fibrinogen by dipping into a 1 mg mL^{-1} fibrinogen solution for 10 minutes, then rinsing in DI water and testing in an artificial perilymph with 1 mg mL^{-1} fibrinogen added. The electrode was also tested in FBS after immersion for 10 minutes.

The OCP of a fibrinogen modified electrode in artificial perilymph with 1 mg mL^{-1} fibrinogen was 141 mV, 76 mV more negative than in the protein free artificial perilymph (Table 1). The voltammetry with fibrinogen in solution was slightly reduced in magnitude and the platinum oxide

reduction peak appeared at -60 mV, more positive than in the absence of fibrinogen in solution (Figure 6). The cathodic CSC was smaller but the anodic CSC was larger with fibrinogen in solution compared to the protein free solution (Table 1).

The chronopotentiometric behaviour was similar in the presence and absence of fibrinogen in solution (Figure 7). The change in potential was slightly smaller with fibrinogen in solution, indicating a larger charge injection capacity (Table 2).

The impedance in the fibrinogen containing artificial perilymph was similar to the solution without fibrinogen and was fitted to the same equivalent circuit (Figure S2). The impedance at 12 Hz and most fitted parameters were the same (Table 3). However there was a significant increase in the polarisation resistance and the standard deviation.

In FBS, the OCP was 64 mV, 53 mV more negative than an FBS modified electrode in artificial perilymph (Table 1). Compared to the FBS modified electrode in artificial perilymph, voltammetry in FBS showed suppression of the platinum oxide reduction peak at -52 mV; the hydrogen adsorption and desorption process was shifted to more positive potentials; and a much larger oxidation current occurred with a shoulder around 550 mV (Figure 6). This response is again consistent with strong adsorption of amino acids on the platinum electrode [34]. However there was no difference in the CSC (Table 1). The chronopotentiometric response and change in potential was also the same with an FBS modified electrode in artificial perilymph and in FBS (Figure 7, Table 2). The impedance was also similar in both solutions, but the polarisation resistance was several orders of magnitude larger in FBS (Figure S2, Table 3).

The impact of protein in solution was seen to reduce the electrode OCP. This is consistent with protein adsorption on the reference electrode shifting the reference potential. The impact on CSC and charge injection capacity was minimal but there was an increase in polarisation resistance indicating poor electron transfer across the electrode-solution interface. There was no evidence of proteins in solution affecting its viscosity and the diffusion coefficient of electroactive species [41].

Effective Electrode area of Platinum Before and After Exposure to Protein Solutions

The above experiments indicated protein adsorption blocks the electrode surface, reducing its effective area. While measurement of effective electrode area by impedance is possible, it requires correct modelling of the response and measurement over a wide frequency range, both conditions may not be achievable. The effective area of an electrode can also be measured by voltammetry of a solution based redox species. $Ru(NH_3)_6^{3+}$ is a highly soluble species that undergoes an outer sphere, reversible, one electron reduction process

$$\mathrm{Ru(NH_3)_6^{3+} + e^- \rightleftharpoons Ru(NH_3)_6^{2+}}$$

At fast voltammetric scan rates, the current peak (i_p) associated with the reduction process is related to electrode area (A) by

$$i_p = (2.69\times10^5)n^{3/2}AD^{1/2}C\upsilon^{1/2} \quad (6)$$

where n is the number of electrons transferred, D is the diffusion coefficient (9.0×10^{-6} cm^2 s^{-1}), C is the concentration and ν is the voltammetric scan rate [21]. Voltammetry of a freshly polished platinum electrode in artificial perilymph with 5.1 mM $Ru(NH_3)_6^{3+}$ at a scan rate of 100 mV s^{-1} displayed well resolved reduction and oxidation peaks at -210 mV and -142 mV respectively, giving a peak separation (ΔE) of 68 mV and a mid-point potential of -176 mV (Figure 8). The cathodic peak current was 2.9 µA and the anodic 3.3 µA, giving an electrode area of 2.55 x 10^{-3} cm^2. The response at pH 5.5 at the same scan rate was identical. If protein adsorption blocked a large continuous region of the electrode, then the effective area would decrease, lowering the peak current. However the response of $Ru(NH_3)_6^{3+}$ on electrodes exposed to protein solutions at 100 mV s^{-1} was indistinguishable from the pristine electrodes. This indicates electrode blocking is occurring on smaller, non-continuous regions [42].

Diffusion layer thickness (δ) is a function of time (t) with $\delta = \sqrt{2Dt}$. In voltammetry, t is estimated to be $1/\nu$, so at a scan rate of 100 mV s^{-1} the diffusion length of $Ru(NH_3)_6^{3+}$ is approximately 134 µm. At this scan rate, the diffusion layer of active regions of a partially blocked electrode separated by less than 134 µm would overlap. Voltammetry of $Ru(NH_3)_6^{3+}$ on platinum exposed to protein at 100 mV s^{-1} showed minimal impact, indicating protein blocking domains are significantly smaller than 134 µm. The $Ru(NH_3)_6^{3+}$ above the blocking protein can diffuse to active regions of the electrode, so the protein blocks are essentially invisible. Increasing the scan rate reduces the diffusion length, so at a scan rate of 10 V s^{-1}, the diffusion length becomes ~13 µm. At this scan rate, differences in response between unmodified platinum and after protein adsorption can be seen (Figure 8). There is a general reduction in the peak current and an increase in peak splitting (Table 4). A similar response was seen for the voltammetry of ferrocyanide on a platinum electrode after adsorption of BSA, fibrinogen or bovine serum, but no analysis of the response was undertaken [43]. Some publications have taken the response after protein adsorption to be due to a reduction in electron transfer rate (k_0) [23][24]. However the dimensions of individual proteins are ~4-40 nm, while tunnelling rate decreases exponentially with distance, becoming negligible at distances greater than ~1.5 nm [44]. Compacted and unfolded proteins also have dimensions greater than the maximum tunnelling distance. Furthermore, if protein adsorption reduced the electron transfer rate on part of the electrode, then voltammograms would display 2 reduction and oxidation peaks emerging at high scan rates; one set from the unblocked electrode with a high charge transfer rate and one from the blocked region with a

lower charge transfer rate [42]. A distribution of slow electron transfer rates from varying thicknesses of adsorbing material would appear as a broadening of the redox peaks. Only one set of redox peaks were seen, and no peak broadening was observed, therefore regions coated by protein were completely blocked to electron transfer. Even proteins containing redox centres completely block the electrode surface [45]. The apparent decrease in rate constant is due to partial blocking of small domains on a larger electrode [25][26]. The $Ru(NH_3)_6^{3+}$ has a mixed diffusion profile towards the unblocked electrode regions. Diffusion will be linear directly above the unblocked electrode and radial from regions above blocking protein towards unblocked electrode. Under conditions where there is heavy overlap of diffusion layers from unblocked regions, the apparent rate constant (k_{ap}) is related to the fractional block coverage (θ),

$$k_{ap} = k_0 (1- \theta) \quad (7)$$

This relationship only holds where there is heavy overlap of diffusion layers between unblocked regions. The thickness of the blocking layer also impacts the response. If the diffusion length is smaller than the blocking layer height, diffusion to the unblocked regions will be linear; when the diffusion length is greater than the blocking layer height, the mixed radial and linear diffusion profile occurs [46]. In the present case, the protein height is significantly smaller than the diffusion length and a mixed diffusion profile occurs at all measured scan rates. At very high θ, diffusion to the electrode would occur through small pinholes. The voltametric response through pinholes is scan rate dependant, displaying a planar 1 dimensional response at high scan rates and a steady state response at slow scan rates [47]. No steady state behaviour was observed in the present work, indicating current passage from diffusion through pinholes is minimal.

Fitting of the voltammetric response of $Ru(NH_3)_6^{3+}$ using DigiElch was good for the unmodified platinum, but was poor after protein adsorption. The simulations are unable to properly account for the complex diffusion profile at a partially blocked electrode. Estimates of k_{ap} were made by the best fit possible, producing an i_p versus $\nu^{1/2}$ curve similar to the protein modified electrodes and calculation of a θ via equation 7 of ~0.57. More accurate measures of θ can be made using 2 dimensional modelling with mixed diffusion rather than the single diffusion model available in DigiElch [42].

4. Discussion

General Considerations of Charge Transfer Mechanisms Following Protein Fouling

Proteins have been shown to adsorb onto an electrode, impacting charge transfer across the electrode-solution interface [31]. This raises concerns of the effect of protein fouling on implantable electrodes on the safe electrical stimulation of electrically excitable cells, the measurement of electrophysiological signals, electrode corrosion, power usage, and the relevance of preclinical testing in simple electrolyte solutions.

Ideally, testing electrodes in simple electrolytes would reduce the resistance (R_u) of a solution, enabling current flow without ohmic drop (iR_u). The electrolyte would also be stable and not interact with the electrode. In reality electrolytes can undergo reactions such as the oxidation of Cl^- to chlorine gas, and they can interact with the electrode such as anion adsorption onto platinum. Understanding charge transfer at an implantable electrode therefore requires a relevant electrolyte composition. We have previously shown the electrode surface and applied waveform also affect the charge transfer mechanisms [17][18][19]. Studies investigating new waveforms, electrode materials or their stability can only provide useful information when performed under relevant conditions. The impact of protein adsorption onto an electrode must be understood, so that more relevant testing conditions for new electrode materials and waveforms can be used.

Electrodes placed into solution without current flow will be at their OCP. Under certain conditions, this will be stable and at equilibrium, but typically electrodes will not be at equilibrium and the OCP will change over time and with conditions. The OCP of a platinum electrode in AP will depend on the concentration of H^+, OH^-, O_2, the electrolyte composition, anion adsorption and subsequently temperature, pressure, etc. It is also measured versus a reference electrode, in this case a Ag/AgCl (3M KCl) electrode with a porous glass frit. Electrodes placed in the body will be surrounded by a complex media which is far from stable and equilibrium, and the reference electrode is typically a large platinum electrode. The OCP of electrodes exposed to individual proteins was seen to move to more positive potentials, which is due to electron withdrawing effects, but the more complex FBS shifted to more negative potentials indicating electron donation. This is most likely due to adsorption of polar or charged species onto the electrode surface and rearrangement of the electrical double layer rather than charge transfer from Faradaic reactions. FBS contains many species not present in the individual protein solution including growth hormones, lipids, amino acids and sugars. The negative OCP shift in FBS is likely due to adsorption of certain electron donating species onto platinum, such as cysteine [34]. Protein adsorption also likely occurred onto the reference electrode, shifting the reference potential. A similar effect was seen when protein adsorbed onto the reference electrode of a voltammetric ion selective electrode [48].

While there were small movements in OCP after fouling, all of the conditions tested here kept it within the platinum oxide region. Therefore the charge transfer mechanisms occurring during current pulsing from these starting conditions are mostly associated with capacitance, platinum oxide reduction and oxidation and anion adsorption. However Faradaic reactions of proteins, amino acids and other organics may also occur [34]. Protein adsorption also alters the structure of the electrode-solution interface including ion rearrangement and changes in local pH which may affect the charge transfer reactions occurring [49]. The OCP of an electrode, its change in potential and charge transfer mechanisms will therefore depend on tissue composition and its location in the body. A significant

change in OCP may result in charge being passed through other reactions such as the oxidation and reduction of water.

When current passes through an electrode, charge is supplied by capacitance and Faradaic reactions. Capacitance is due to the rearrangement of ions in the electrical double layer over active regions of the electrode while Faradaic reactions can be associated with dissolved redox species or the electrode surface. The amount of capacitance and Faradaic charge that passes through an electrode is a function of its area. Partial blocking of an electrode surface reduces its active electrode area and its capacitance. The amount of Faradaic charge passed through a partially blocked electrode depends on the blocking geometry and time.

The CSC of an electrode is typically measured to assess the safe level of charge that it can pass. In general there was a decrease in CSC after protein fouling, mainly due to a reduction in effective area. At lower pH, the CSC of platinum was also reduced due to less charge associated with the hydrogen adsorption process; however the charge injection capacity was barely affected. This is due to the reaction potential shifting with pH and CSC measured over a fixed reference potential range while charge injection capacity is measured relative to the working electrode potential. However changes in pH can also affect the reaction pathways and their kinetics, for instance the reduction of oxygen can be blocked by OH adsorption [50]. Simply measuring CSC doesn't capture this mechanistic information. The poor correlation between charge injection capacity and CSC, particularly after exposure to FBS, further indicates more complicated mechanisms are occurring.

To understand the impact of pH on protein fouling, fibrinogen adsorption was performed above its isoelectric point and the electrochemical response measured at the isoelectric point. This was done to ensure similar amounts of protein were adsorbed onto the electrode across the experiments. Adsorption of fibrinogen at the isoelectric point may affect the amount of protein adsorbed and its conformation, but this would not affect the overall conclusions of this study and wasn't measured. In the body, negative, positive and neutral proteins will be in close proximity to an implanted electrode. The protein charge, electrode surface properties and other parameters will affect which proteins initially adsorb, and subsequently reconfiguration or displacement by other species will occur [49].

Implications of Protein Fouling at the Electrode/Tissue Interface

It's possible to measure surface adsorption of proteins by a variety of methods, including microscopic techniques or mass adsorption by quartz crystal microbalance. However these methods don't provide information on the effective electrode area, which is important for understanding the impact on charge transfer across the electrode/tissue interface. Impedance can be used to measure the electrode area, but the values may not be accurate or measureable for particular systems. In the current work, the

applied frequency could not be lowered sufficiently to obtain an accurate electrode area. Different voltammetric methods can be used on a wider variety of systems but requires careful application and modelling. The effective area can be calculated from hydrogen adsorption on platinum, but there are issues with its accuracy [17]. This method is also performed at very low pH, which would affect protein adsorption and structure, limiting its utility in assessing protein fouling in biological conditions. Voltammetry of a soluble redox species such as $Ru(NH_3)_6^{3+}$ can be performed in more biologically relevant conditions. However, great care must be taken in analysing the response, for instance the use of equation 6 to calculate an electrode area after protein fouling is not valid, as the diffusion profile is non-linear. Modelling of the response with commercial electrochemical packages like DigiElch are also unable to account for complex diffusion profiles.

In the current work, specific values of partial blockage were ~0.57 after a 10 minute dip coating from individual proteins or FBS. In the body, there are other proteins and fouling species. The amount and type of fouling species adsorbing will change over time and depend on location in the body. The adsorbed species can also migrate across the surface and form aggregates. Higher concentrations and applied potential can enhance protein adsorption [51]. Mixed protein solutions can affect the amount and conformation of adsorption through cooperative effects [52][49]. Increased temperature and changes in pH or ionic strength can also affect the amount and conformation of adsorption, and may denature or gel proteins onto the electrode surface, however these conditions are unlikely to arise in vivo [52]. Charge transfer across the electrode-tissue interface may alter the species adsorbed, including generating new species or denature adsorbed proteins. For instance, deep brain stimulating electrodes are used to control tremor for Parkinson's disease sufferers, but dopamine oxidation leads to its polymerisation and electrode fouling [53]. Therefore, the fractional coverage and geometry of protein fouling (and other species) and the diffusion profile towards a partially blocked electrode will be different on every electrode and change over time.

Electrode pretreatment or different electrode materials have an impact on the amount and type of protein adsorption [23]. These experiments were performed on mechanically polished platinum which is multicrystalline and has an oxide layer present. Acid cleaning of platinum can be performed by potential cycling in H_2SO_4 to remove oxide and organic species. Electrical stimulation of an acid cleaned or oxide free electrode leads to platinum oxidation [38]. Protein adsorption on an acid cleaned platinum electrode displayed a small decrease in charge storage capacity, indicating some electrode blocking occurred [52]. However the platinum underlying the fouling layer is unlikely to undergo oxidation during electrical stimulation.

When applying current to an electrode, the charge density across its surface is non-uniform. Radial diffusion to the edge of an electrode enhances mass transport and increases the local charge density.

When protein fouling partially blocks an electrode, new edges are created across the electrode surface [54]. Subsequently, active regions in the centre of a partially blocked electrode pass a higher charge density than on an unblocked electrode. This could result in enhanced Faradaic current, including platinum dissolution. Studies of platinum dissolution in phosphate buffered saline from an acid cleaned electrode during biphasic current pulsing displayed a constant dissolution rate over time [14]. Addition of human serum albumin had a variable and similar initial dissolution rate, but decreased to very low dissolution rates after several hours of immersion. This is consistent with protein adsorption increasing over time, with θ approaching 1. This results in a resistive layer forming across the electrode surface and considerable iR_u. The polarisation voltage would be very large and very little charge would be attributed to capacitance or Faradaic reactions, including platinum dissolution. However immersion of the electrode in the protein solution for 90 hours before electrical stimulation still displayed the same dissolution curve, indicating protein adsorption is low on the acid cleaned platinum, but high on platinum oxide. Removal of protein from the solution led to desorption of the protein from the electrode surface and an increase in platinum dissolution. In the body, electrodes are not acid cleaned before use and are in constant contact with protein during electrical stimulation. Therefore partial blocking of the electrode will occur immediately on implantation. The amount and rate of protein adsorption will vary in vivo, as will the iR_u. Preclinical testing solutions for an electrode should include proteins to assess its antifouling properties. But the use of an individual protein may not capture cooperation effects or test proteins that have the strongest impact on charge transfer.

Protein adsorption may also affect electrophysiological recording. The impedance of an electrode is related to its thermal noise and signal to noise ratio (SNR) of electrophysiological recording [22]. Low frequency impedance is dependent on the electrode properties and can predict SNR. Following protein fouling, the low frequency impedance increased slightly, which would reduce SNR. Changes in pH and the presence of protein in solution had no effect on low frequency impedance and would have no impact on SNR.

The performance of clinical devices is often assessed by an impedance test. The test varies with device, but typically uses Ohm's law to calculate a resistance value from a biphasic current pulse. While the use of Ohm's law in this setting is not valid, as the electrochemical system is not a uniform conductor, the measurement does provide information on the electrode/tissue interface [20]. Changes to stimulation waveform, electrode structure, size, solution composition, resistance and capacitance have been shown to affect the impedance test [19][20]. Oxidation of platinum increased the electrode capacitance, reducing the impedance test [38]. Now electrode blocking was seen to reduce the effective electrode area, and significantly increase the impedance test. Further work should now investigate the relationship of these factors with power usage and the ability to stimulate and record

electrophysiological activity. Further studies could also assess the degree of electrode blocking occurring after implantation in different tissues and on different electrode materials over varying periods of time [55]. The impact of partial electrode blocking on electrode corrosion [56] and function of biosensors [57] should also be examined.

The impact of partial electrode blocking on charge transfer depends on diffusion length and scan rate (time). Typically electrical stimulation of electrically excitable cells is performed with a current pulse on the order of 25 µs, this would result in a $Ru(NH_3)_6^{3+}$ diffusion length of just 0.2 µm. This would reduce the radial diffusion current, so use of equation 6 to determine the effective electrode area becomes more accurate, but a mixed linear and radial diffusion current would still occur. Achieving this diffusion length through cyclic voltammetry would require a scan rate in the order of 40 kV s^{-1}, which is not achievable with many commercial potentiostats. The size of the blocking species can also be measured through this method. As the dimensions of individual proteins is ~4-40 nm, creating a diffusion length on the scale of individual proteins would require scan rates greater than 100 MV s^{-1}.

5. Conclusions

Proteins can adsorb onto platinum, partially blocking the electrode. Adsorption of species onto an electrode shifts its OCP. Individual proteins shifted the OCP more positive while FBS shifted it more negative, but the OCP remained within the platinum oxide region. In general, protein adsorption reduced the CSC and charge injection capacity of platinum, but there was a poor correlation between the two measurements. Protein adsorption increased the low frequency impedance and fitting an equivalent circuit generally led to an increase in polarisation resistance and decrease in admittance. Effective electrode area measurements made from impedance were inaccurate, as the applied frequency couldn't be lowered sufficiently. The effective electrode area could be assessed by voltammetry of a solution based redox species. Partial electrode blocking appears as a reduced electron transfer rate, but is due to a mixed diffusion profile to active electrode regions. The diffusion profile is time and blocking geometry dependant. The amount and geometry of protein fouling on electrodes in vivo is expected to change over time and location. Protein fouling on an electrode reduces platinum dissolution by increasing Ohmic drop and reducing charge available for Faradaic reactions. Electrode testing for preclinical trials should include protein in the test solution to assess its antifouling performance.

Acknowledgements

The authors acknowledge the financial support of the HEARing CRC, established under the Australian Government's Cooperative Research Centres (CRC) Program. The CRC Program supports industry-led collaborations between industry, researchers and the community. Funding from the Australian Research Council Centre of Excellence Scheme (Project Number CE140100012) is gratefully acknowledged.

References

[1] G.M. Clark, Y.C. Tong, Multiple-electrode cochlear implant for profound or total hearing loss: a review, Med. J. Aust. 18 (1981) 428–429.

[2] M.J. Cook, T.J. O'Brien, S.F. Berkovic, M. Murphy, A. Morokoff, G. Fabinyi, W. D'Souza, R. Yerra, J. Archer, L. Litewka, S. Hosking, P. Lightfoot, V. Ruedebusch, W.D. Sheffield, D. Snyder, K. Leyde, D. Himes, Prediction of seizure likelihood with a long-term, implanted seizure advisory system in patients with drug-resistant epilepsy: a first-in-man study, Lancet Neurol. 12 (2013) 563–571. https://doi.org/http://dx.doi.org/10.1016/S1474-4422(13)70075-9.

[3] E. Kocabicak, Y. Temel, Deep brain stimulation of the subthalamic nucleus in Parkinson's disease: Surgical technique, tips, tricks and complications, Clin. Neurol. Neurosurg. 115 (2013) 2318–2323. https://doi.org/http://dx.doi.org/10.1016/j.clineuro.2013.08.020.

[4] S.J. Kanowitz, W.H. Shapiro, J.G. Golfinos, N.L. Cohen, J.T. Roland, Auditory brainstem implantation in patients with neurofibromatosis type 2, Laryngoscope. 114 (2004) 2135–2146. https://doi.org/10.1097/01.mlg.0000149447.52888.f6.

[5] C.N. Shealy, J.T. Mortimer, J.B. Reswick, Electrical Inhibition of Pain by Stimulation of the Dorsal Columns: Preliminary Clinical Report, Anesth. Analg. 46 (1967). https://journals.lww.com/anesthesia-analgesia/Fulltext/1967/07000/Electrical_Inhibition_of_Pain_by_Stimulation_of.25.aspx.

[6] C.C. Horn, J.L. Ardell, L.E. Fisher, Electroceutical Targeting of the Autonomic Nervous System, Physiology. 34 (2019) 150–162. https://doi.org/10.1152/physiol.00030.2018.

[7] A.T. Chuang, C.E. Margo, P.B. Greenberg, Retinal implants: a systematic review, Br. J. Ophthalmol. 98 (2014) 852 LP – 856. https://doi.org/10.1136/bjophthalmol-2013-303708.

[8] A.R. Harris, Current perspectives on the safe electrical stimulation of peripheral nerves with platinum electrodes, Bioelectron. Med. 3 (2020) 37–49. https://doi.org/10.2217/bem-2020-0007.

[9] S.F. Cogan, Neural Stimulation and Recording Electrodes, Annu. Rev. Biomed. Eng. 10 (2008) 275–309. https://doi.org/doi:10.1146/annurev.bioeng.10.061807.160518.

[10] S.B. Brummer, M.J. Turner, Electrical stimulation of the nervous system: The principle of safe charge injection with noble metal electrodes, Bioelectrochemistry Bioenerg. 2 (1975) 13–25. https://doi.org/Doi: 10.1016/0302-4598(75)80002-x.

[11] S.B. Brummer, M.J. Turner, Electrical Stimulation with Pt Electrodes: II-Estimation of Maximum Surface Redox (Theoretical Non-Gassing) Limits, Biomed. Eng. IEEE Trans. BME-24 (1977) 440–443.

[12] S.B. Brummer, J. McHardy, M.J. Turner, Electrical stimulation with Pt electrodes: trace analysis for dissolved platinum and other dissolved electrochemical products, Brain. Behav. Evol. 14 (1977) 10–22.

[13] J. McHardy, L.S. Robblee, J.M. Marston, S.B. Brummer, Electrical stimulation with Pt electrodes. IV. Factors influencing Pt dissolution in inorganic saline, Biomaterials. 1 (1980) 129–134. https://doi.org/Doi: 10.1016/0142-9612(80)90034-4.

[14] L.S. Robblee, J. McHardy, J.M. Marston, S.B. Brummer, Electrical stimulation with Pt electrodes. V. The effect of protein on Pt dissolution, Biomaterials. 1 (1980) 135–139. https://doi.org/Doi: 10.1016/0142-9612(80)90035-6.

[15] L.S. Robblee, J. McHardy, W.F. Agnew, L.A. Bullara, Electrical stimulation with Pt electrodes. VII. Dissolution of Pt electrodes during electrical stimulation of the cat cerebral

cortex, J. Neurosci. Methods. 9 (1983) 301–308. https://doi.org/10.1016/0165-0270(83)90062-6.
[16] W.F. Agnew, T.G.H. Yuen, D.B. McCreery, L.A. Bullara, Histopathologic evaluation of prolonged intracortical electrical stimulation, Exp. Neurol. 92 (1986) 162–185. https://doi.org/Doi: 10.1016/0014-4886(86)90132-9.
[17] A.R. Harris, C. Newbold, P. Carter, R. Cowan, G.G. Wallace, Measuring the Effective Area and Charge Density of Platinum Electrodes for Bionic Devices, J. Neural Eng. 15 (2018) 46015. https://doi.org/doi.org/10.1088/1741-2552/aaba8b.
[18] A.R. Harris, C. Newbold, P. Carter, R. Cowan, G.G. Wallace, Charge Injection from Chronoamperometry of Platinum Electrodes for Bionic Devices, J. Electrochem. Soc. 165 (2018) G3033–G3041. https://doi.org/10.1149/2.0101812jes.
[19] A.R. Harris, C. Newbold, P. Carter, R. Cowan, G.G. Wallace, Using Chronopotentiometry to Better Characterize the Charge Injection Mechanisms of Platinum Electrodes Used in Bionic Devices, Front. Neurosci. 13 (2019) 380. https://doi.org/10.3389/fnins.2019.00380.
[20] A.R. Harris, C. Newbold, R. Cowan, G.G. Wallace, Insights into the Electron Transfer Kinetics, Capacitance and Resistance Effects of Implantable Electrodes Using Fourier Transform AC Voltammetry on Platinum, J. Electrochem. Soc. . 166 (2019) G131–G140. https://doi.org/10.1149/2.1361910jes.
[21] A.R. Harris, P.J. Molino, R.M.I. Kapsa, G.M. Clark, A.G. Paolini, G.G. Wallace, Optical and Electrochemical Methods for Determining the Effective Area and Charge Density of Conducting Polymer Modified Electrodes for Neural Stimulation, Anal. Chem. 87 (2014) 738–746. https://doi.org/10.1021/ac503733s.
[22] A.R. Harris, B. Allitt, A. Paolini, Predicting Neural Recording Performance of Implantable Electrodes, Analyst. 144 (2019) 2973–2983. https://doi.org/10.1039/c8an02214c.
[23] A.J. Downard, A.D. Roddick, Effect of electrochemical pretreatment on protein adsorption at glassy carbon electrodes protein, Electroanalysis. 6 (1994) 409–414. https://doi.org/10.1002/elan.1140060509.
[24] S.E. Moulton, J.N. Barisci, A. Bath, R. Stella, G.G. Wallace, Investigation of protein adsorption and electrochemical behavior at a gold electrode, J. Colloid Interface Sci. 261 (2003) 312–319. https://doi.org/10.1016/s0021-9797(03)00073-0.
[25] C. Amatore, J.M. Saveant, D. Tessier, Charge transfer at partially blocked surfaces: A model for the case of microscopic active and inactive sites, J. Electroanal. Chem. 147 (1983) 39–51. http://www.sciencedirect.com/science/article/B6TGB-4K7KHTJ-3/2/080cdc8e7c07f7228e3f415c67c36530.
[26] T. Davies, C. Banks, R. Compton, Voltammetry at spatially heterogeneous electrodes, J. Solid State Electrochem. 9 (2005) 797–808. https://doi.org/10.1007/s10008-005-0699-x.
[27] A.N. Salt, C. Kellner, S. Hale, Contamination of perilymph sampled from the basal cochlear turn with cerebrospinal fluid, Hear. Res. 182 (2003) 24–33. https://doi.org/http://dx.doi.org/10.1016/S0378-5955(03)00137-0.
[28] S.F. Cogan, K.A. Ludwig, C.G. Welle, P. Takmakov, Tissue damage thresholds during therapeutic electrical stimulation, J. Neural Eng. 13 (2016) 21001. http://stacks.iop.org/1741-2552/13/i=2/a=021001.
[29] A.C. Lysaght, S.-Y. Kao, J.A. Paulo, S.N. Merchant, H. Steen, K.M. Stankovic, Proteome of human perilymph, J. Proteome Res. 10 (2011) 3845–3851. https://doi.org/10.1021/pr200346q.
[30] J. Selvakumaran, J.L. Keddie, D.J. Ewins, M.P. Hughes, Protein adsorption on materials for recording sites on implantable microelectrodes, J. Mater. Sci. Mater. Med. 19 (2008) 143–151.
[31] Z. Yue, P.J. Molino, X. Liu, G.G. Wallace, PEGylation of platinum bio-electrodes, Electrochem. Commun. 27 (2013) 54–58. https://doi.org/https://doi.org/10.1016/j.elecom.2012.11.007.
[32] J.C. Palmer, M.S. Lord, J.L. Pinyon, A.K. Wise, N.H. Lovell, P.M. Carter, Y.L. Enke, G.D. Housley, R.A. Green, Comparing perilymph proteomes across species, Laryngoscope. 128 (2018) E47–E52. https://doi.org/10.1002/lary.26885.
[33] T. Peters, Serum Albumin, in: C.B. Anfinsen, J.T. Edsall, F.M.B.T.-A. in P.C. Richards (Eds.), Adv. Protein Chem., Academic Press, 1985: pp. 161–245. https://doi.org/10.1016/S0065-3233(08)60065-0.

[34] D.B. Hibbert, K. Weitzner, P. Carter, Voltammetry of Platinum in Artificial Perilymph Solution, J. Electrochem. Soc. 148 (2001) E1–E7. https://doi.org/10.1149/1.1344543.
[35] D.R. Merrill, M. Bikson, J.G.R. Jefferys, Electrical stimulation of excitable tissue: design of efficacious and safe protocols, J. Neurosci. Methods. 141 (2005) 171–198. https://doi.org/DOI: 10.1016/j.jneumeth.2004.10.020.
[36] W. Franks, I. Schenker, P. Schmutz, A. Hierlemann, Impedance characterization and modeling of electrodes for biomedical applications, Biomed. Eng. IEEE Trans. 52 (2005) 1295–1302.
[37] T. Pajkossy, Impedance of rough capacitive electrodes, J. Electroanal. Chem. 364 (1994) 111–125. https://doi.org/https://doi.org/10.1016/0022-0728(93)02949-I.
[38] A. Harris, Understanding Charge Transfer on the Clinically Used Conical Utah Electrode Array: Charge Storage Capacity, Electrochemical Impedance Spectroscopy and Effective Electrode Area, J. Neural Eng. (2021) In Press. https://doi.org/10.1088/1741-2552/abd897.
[39] C.H. Hsu, F. Mansfeld, Technical Note: Concerning the Conversion of the Constant Phase Element Parameter Y0 into a Capacitance, Corrosion. 57 (2001) 2. https://doi.org/.
[40] P. Bernabeu, L. Tamisier, A. De Cesare, A. Caprani, Study of the adsorption of albumin on a platinum rotating disk electrode using impedance measurements, Electrochim. Acta. 33 (1988) 1129–1136. https://doi.org/https://doi.org/10.1016/0013-4686(88)80204-4.
[41] H.-Y. Kim, J. Lee, S. Song, I. Kang, S.Y. Kim, B.-K. Kim, Simple method to analyze the molecular weight of polymers using cyclic voltammetry, Sensors Actuators B Chem. 330 (2021) 129305. https://doi.org/https://doi.org/10.1016/j.snb.2020.129305.
[42] T.J. Davies, R.R. Moore, C.E. Banks, R.G. Compton, The cyclic voltammetric response of electrochemically heterogeneous surfaces, J. Electroanal. Chem. 574 (2004) 123–152. https://doi.org/https://doi.org/10.1016/j.jelechem.2004.07.031.
[43] J. Kuhlmann, L.C. Dzugan, W.R. Heineman, Comparison of the Effects of Biofouling on Voltammetric and Potentiometric Measurements, Electroanalysis. 24 (2012) 1732–1738. https://doi.org/10.1002/elan.201200194.
[44] A.J. Bard, L.R. Faulkner, Electrochemical Methods, 2nd ed., Wiley, New York, 2001.
[45] F.N. Büchi, A.M. Bond, Interpretation of the electrochemistry of cytochrome c at macro and micro sized carbon electrodes using a microscopic model based on a partially blocke, J. Electroanal. Chem. Interfacial Electrochem. 314 (1991) 191–206. https://doi.org/https://doi.org/10.1016/0022-0728(91)85437-T.
[46] F.G. Chevallier, T.J. Davies, O. V Klymenko, L. Jiang, T.G.J. Jones, R.G. Compton, Numerical simulation of partially blocked electrodes under cyclic voltammetry conditions: influence of the block unit geometry on the global electrochemical properties, J. Electroanal. Chem. 577 (2005) 211–221. https://doi.org/https://doi.org/10.1016/j.jelechem.2004.11.033.
[47] D. Menshykau, R.G. Compton, Electrodes Modified with Electroinactive Layers: Distinguishing Through-Film Transport from Pinhole (Pore) Diffusion, Langmuir. 25 (2009) 2519–2529. https://doi.org/10.1021/la803488t.
[48] A.R. Harris, J. Zhang, R.W. Cattrall, A.M. Bond, Applications of voltammetric ion selective electrodes to complex matrices, Anal. Methods. 5 (2013). https://doi.org/10.1039/c3ay40769a.
[49] M. Rabe, D. Verdes, S. Seeger, Understanding protein adsorption phenomena at solid surfaces, Adv. Colloid Interface Sci. 162 (2011) 87–106. https://doi.org/https://doi.org/10.1016/j.cis.2010.12.007.
[50] N.M. Marković, T.J. Schmidt, V. Stamenković, P.N. Ross, Oxygen Reduction Reaction on Pt and Pt Bimetallic Surfaces: A Selective Review, Fuel Cells. 1 (2001) 105–116. https://doi.org/10.1002/1615-6854(200107)1:2<105::AID-FUCE105>3.0.CO;2-9.
[51] J.I. Anzai, B. Guo, T. Osa, Electrochemically accelerated adsorption of serum albumin on the surface of platinum and gold electrodes, Chem. Pharm. Bull. 42 (1994) 2391–2393. https://doi.org/10.1248/cpb.42.2391.
[52] R. Rouhana, S.M. Budge, S.M. Macdonald, S.G. Roscoe, Electrochemical studies of the interfacial behaviour of α-lactalbumin and bovine serum albumin, Food Res. Int. 30 (1997) 13–20. https://doi.org/https://doi.org/10.1016/S0963-9969(96)00014-2.
[53] W. Harreither, R. Trouillon, P. Poulin, W. Neri, A.G. Ewing, G. Safina, Carbon Nanotube Fiber Microelectrodes Show a Higher Resistance to Dopamine Fouling, Anal. Chem. 85 (2013) 7447–7453. https://doi.org/10.1021/ac401399s.

[54] J.C. Myland, K.B. Oldham, The electrochemistry of electrode edges and its relevance to partially blocked voltammetric electrodes, J. Solid State Electrochem. 13 (2009) 521–535. https://doi.org/10.1007/s10008-008-0713-1.
[55] A.R. Harris, G.G. Wallace, Organic Electrodes and Communications with Excitable Cells, Adv. Funct. Mater. 28 (2018) 1700587. https://doi.org/10.1002/adfm.201700587.
[56] N. Eliaz, Corrosion of Metallic Biomaterials: A Review, Mater. (Basel, Switzerland). 12 (2019) 407. https://doi.org/10.3390/ma12030407.
[57] E.T.S.G. da Silva, D.E.P. Souto, J.T.C. Barragan, J. de F. Giarola, A.C.M. de Moraes, L.T. Kubota, Electrochemical Biosensors in Point-of-Care Devices: Recent Advances and Future Trends, ChemElectroChem. 4 (2017) 778–794. https://doi.org/https://doi.org/10.1002/celc.201600758.

Table 1. Open Circuit Potential and charge storage capacity of a mechanically polished platinum electrode after varying protein adsorption.

Protein	Solution	pH	Open Circuit Potential /mV	Charge Storage Capacity /μC	
				Reduction Sweep	Oxidation Sweep
-	AP	8.1	146 (18)	5.3 (0.2)	4.5 (0.6)
BSA	AP	8.1	230 (6)	5.7 (0.7)	3.3 (0.1)
Fibrinogen	AP	8.1	217 (4)	5.0 (0.2)	3.1 (0.4)
Trypsin Inhibitor	AP	8.1	219 (6)	4.2 (0.2)	3.7 (0.1)
FBS	AP	8.1	117 (2)	4.6 (0.2)	4.4 (0.2)
-	AP	5.5	134 (4)	3.7 (0.1)	3.4 (0.1)
Fibrinogen	AP	5.5	217 (4)	4.2 (0.3)	2.6 (0.2)
Fibrinogen	1 mg/mL Fibrinogen in AP	8.1	141 (5)	4.3 (0.1)	3.8 (0.3)
FBS	FBS	-	64 (19)	4.5 (0.1)	4.6 (0.2)

Average (standard deviation) of 3 repetitions

Table 2. Change in potential of a mechanically polished platinum electrode with a 5 ms pulse at 10 μC cm^{-2} after varying protein adsorption.

Protein	Solution	pH	Initial Applied Pulse Polarity	Change in Potential /mV	
				Second Pulse	Cumulative 6 Pulses
-	AP	8.1	Cathodic	237 (22)	25 (3)
-	AP	8.1	Anodic	-218 (17)	-21 (3)
BSA	AP	8.1	Cathodic	256 (14)	24 (1)
BSA	AP	8.1	Anodic	-265 (7)	-22 (2)
Fibrinogen	AP	8.1	Cathodic	328 (14)	31 (2)
Fibrinogen	AP	8.1	Anodic	-349 (22)	-27 (2)
Trypsin Inhibitor	AP	8.1	Cathodic	329 (16)	31 (1)
Trypsin Inhibitor	AP	8.1	Anodic	-316 (17)	-27 (3)
FBS	AP	8.1	Cathodic	401 (17)	41 (2)
FBS	AP	8.1	Anodic	-365 (5)	-39 (2)
-	AP	5.5	Cathodic	213 (10)	24 (2)
-	AP	5.5	Anodic	-218 (23)	-21 (4)
Fibrinogen	AP	5.5	Cathodic	263 (19)	29 (2)
Fibrinogen	AP	5.5	Anodic	-338 (43)	-29 (3)
Fibrinogen	1 mg/mL Fibrinogen in AP	8.1	Cathodic	301 (27)	27 (2)
Fibrinogen	1 mg/mL Fibrinogen in AP	8.1	Anodic	-272 (9)	-24 (1)
FBS	FBS	-	Cathodic	407 (10)	43 (2)
FBS	FBS	-	Anodic	-378 (10)	-47 (1)

Average (standard deviation) of 3 repetitions

Table 3. Electrochemical impedance parameters from equivalent circuit fitting of a mechanically polished platinum electrode after varying protein adsorption.

Protein	Solution	pH	Impedance 12 Hz /kOhm	Solution Resistance /Ohm	Polarisation Resistance /MOhm	Q_0 /10^{-9} S $s^{1/2}$	n	χ^2
-	AP	8.1	85 (8)	839 (17)	2.66 (0.6)	281 (12)	0.86 (0.01)	0.001
BSA	AP	8.1	101 (10)	777 (5)	1.67 (0.5)	252 (24)	0.84 (0.01)	0.001
Fibrinogen	AP	8.1	103 (11)	565 (9)	2.68 (0.3)	253 (34)	0.84 (0.01)	0.001
Trypsin Inhibitor	AP	8.1	120 (5)	488 (16)	10.3 (1.2)	227 (6)	0.83 (0.01)	0.001
FBS	AP	8.1	163 (4)	478 (1)	28 (2.1)	119 (2)	0.91 (0.01)	0.001
-	AP	5.5	85 (5)	637 (32)	5.33 (2.2)	263 (10)	0.87 (0.01)	0.001
Fibrinogen	AP	5.5	99 (12)	537 (115)	1.86 (0.1)	273 (27)	0.83 (0.01)	0.001
Fibrinogen	1 mg/mL Fibrinogen in AP	8.1	101 (17)	775 (69)	17.4 (15.7)	245 (42)	0.86 (0.01)	0.002
FBS	FBS	-	174 (18)	881 (120)	3.9×10^{13} (5.3×10^{13})	113 (14)	0.91 (0.01)	0.003

Average (standard deviation) of 3 repetitions

Table 4. Voltammetric response of 5.1 mM $Ru(NH_3)_6^{3+}$ on bare and protein modified platinum electrodes at a scan rate of 200mV s^{-1} and 10 V s^{-1}.

Protein	pH	200mV s^{-1}		10 V s^{-1}	
		ΔE /mV	Anodic i_p /uA	ΔE /mV	Anodic i_p /uA
-	8.1	69	7.0	120	27.1
BSA	8.1	70	7.2	127	26.0
Fibrinogen	8.1	80	6.8	148	22.2
Trypsin Inhibitor	8.1	80	6.6	146	21.6
FBS	8.1	71	7.0	120	26.0
-	5.5	68	7.4	108	29.6
Fibrinogen	5.5	72	7.3	122	25.2

Average of 3 repetitions

Figure Captions

Figure 1. Second cycle of a cyclic voltammogram in degassed artificial perilymph of a mechanically polished 0.6 mm diameter platinum electrode unmodified or with adsorbed protein at 100 mV s^{-1}.

Figure 2. Multiple pulse chronopotentiometry of a mechanically polished 0.6 mm diameter platinum electrode unmodified or with adsorbed protein in degassed artificial perilymph. (a) Cathodic, (b) anodic pulse first with a current density of 10 µC cm^{-2}.

Figure 3. Electrochemical impedance spectroscopy of a mechanically polished 0.6 mm diameter platinum electrode unmodified or with adsorbed protein in degassed artificial perilymph at 0 V with an ac amplitude of 5 mV and the equivalent circuit used to fit the data.

Figure 4. Second cycle of a cyclic voltammogram in degassed artificial perilymph at pH 5.5 of a mechanically polished 0.6 mm diameter platinum electrode unmodified or with fibrinogen at 100 mV s^{-1}.

Figure 5. Multiple pulse chronopotentiometry of a mechanically polished 0.6 mm diameter platinum electrode unmodified or with adsorbed fibrinogen in degassed artificial perilymph at pH 5.5. (a) Cathodic, (b) anodic pulse first with a current density of 10 µC cm^{-2}.

Figure 6. Second cycle of a cyclic voltammogram of a mechanically polished 0.6 mm diameter platinum electrode in degassed artificial perilymph with 1 mg mL^{-1} fibrinogen or in FBS at 100 mV s^{-1}.

Figure 7. Multiple pulse chronopotentiometry of a mechanically polished 0.6 mm diameter platinum electrode in degassed artificial perilymph with 1 mg mL^{-1} fibrinogen or in FBS. (a) Cathodic, (b) anodic pulse first with a current density of 10 µC cm^{-2}.

Figure 8. (a) Second cycle of a cyclic voltammogram in degassed artificial perilymph with 5.1 mM $Ru(NH_3)_6^{3+}$ on a mechanically polished 0.6 mm diameter platinum electrode unmodified or with adsorbed protein at 10 V s^{-1}. (b) Peak current of the oxidation of $Ru(NH_3)_6^{3+}$ with no background subtraction; fitted curve calculated from best fit possible from DigiElch simulations and calculation of θ via equation 7.

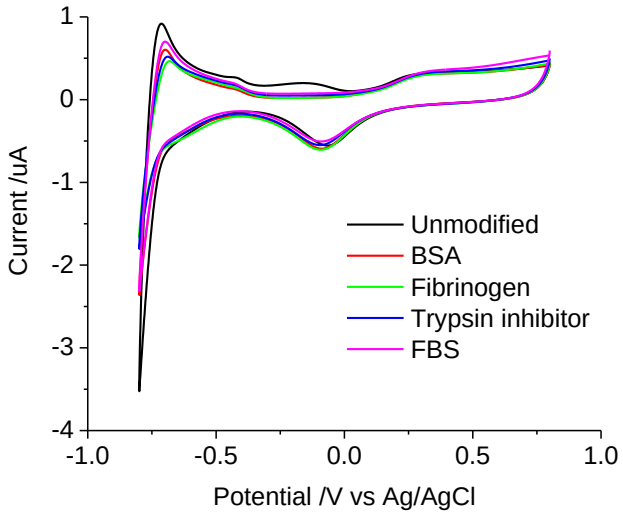

Figure 1

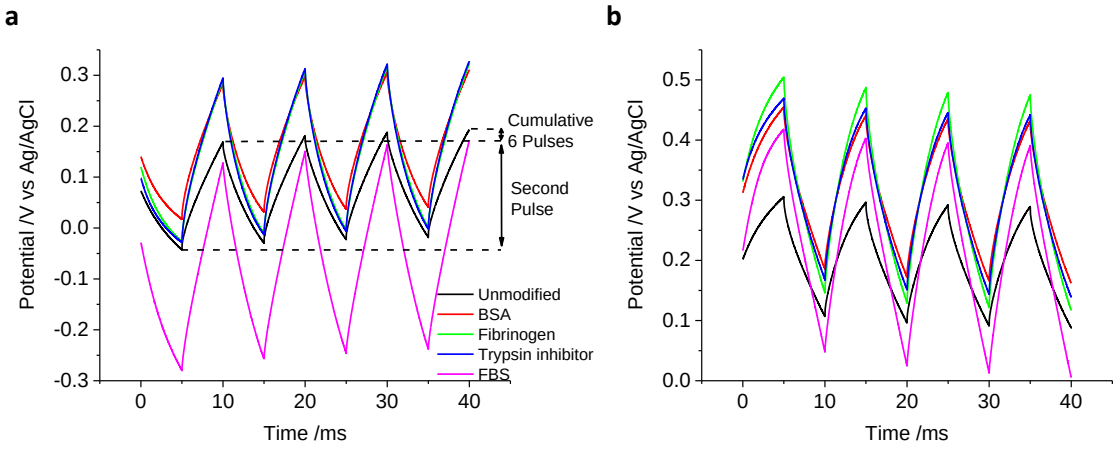

Figure 2

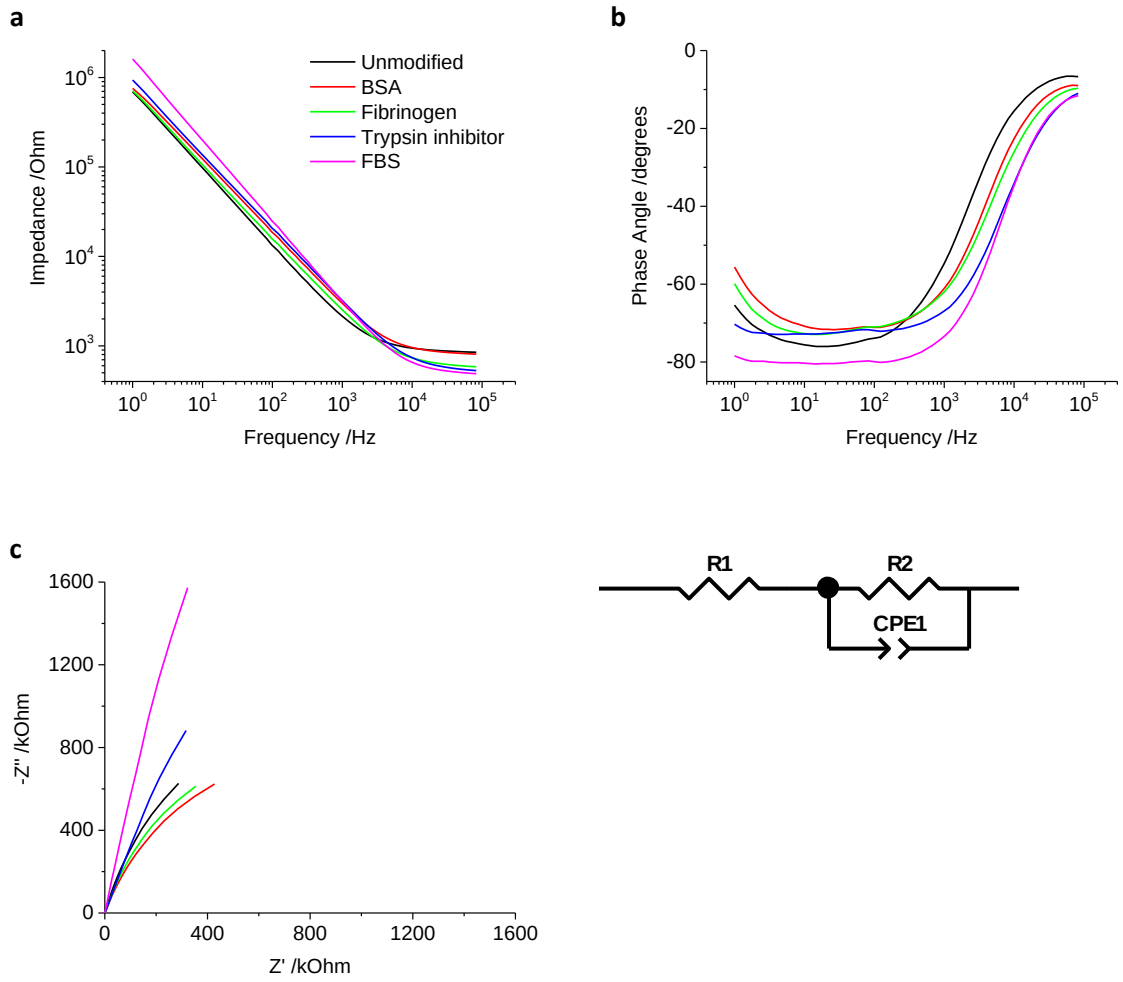

Figure 3

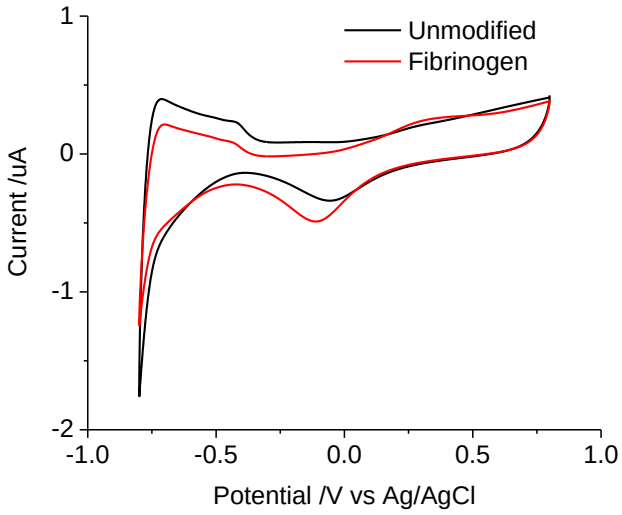

Figure 4

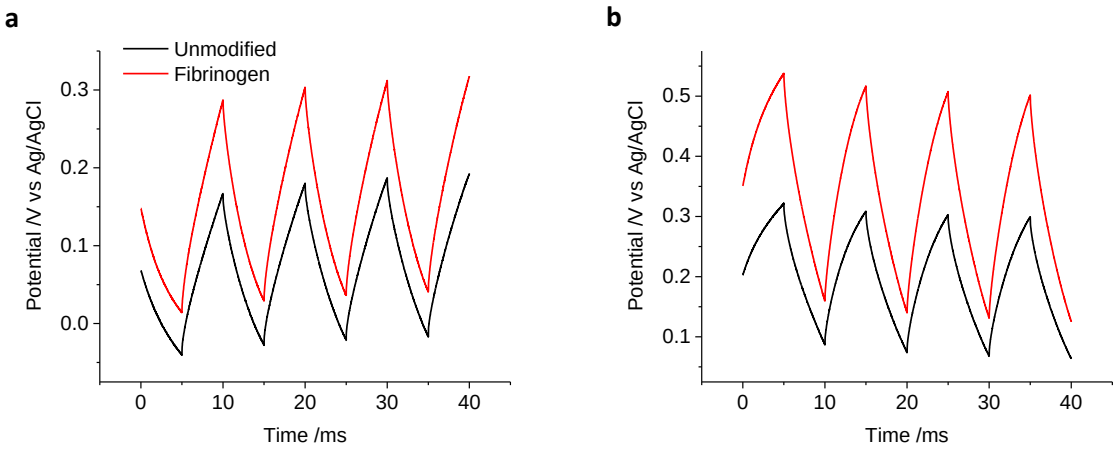

Figure 5

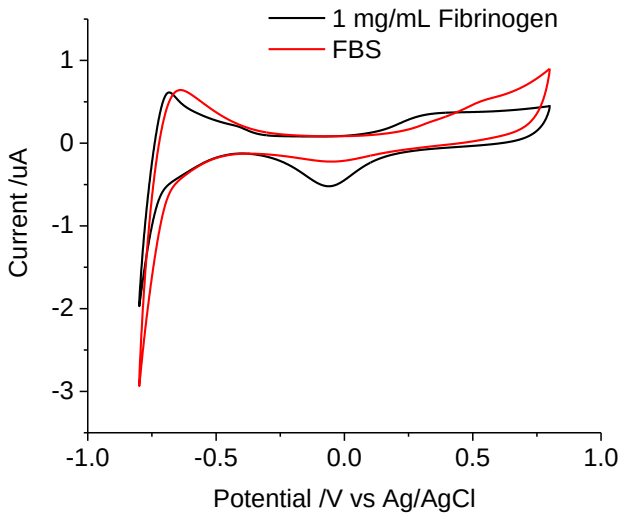

Figure 6

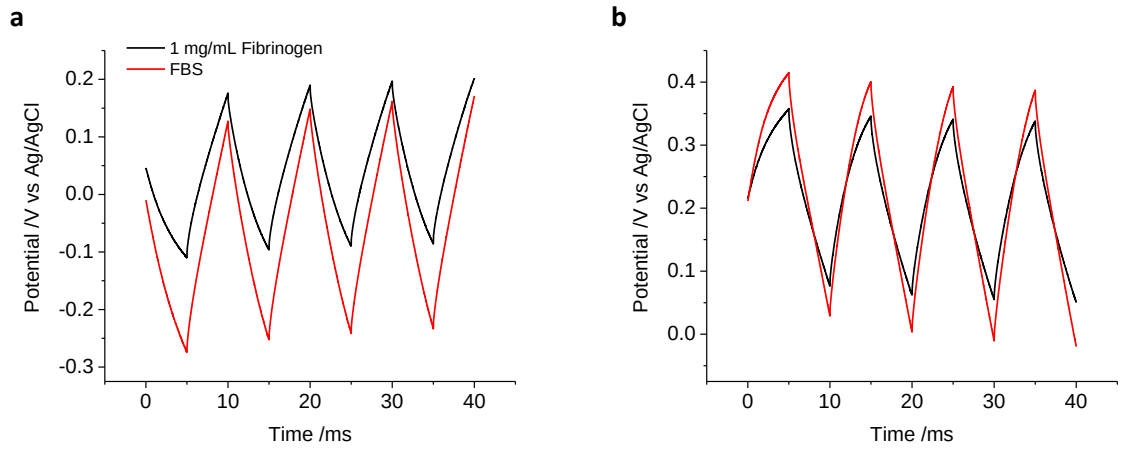

Figure 7

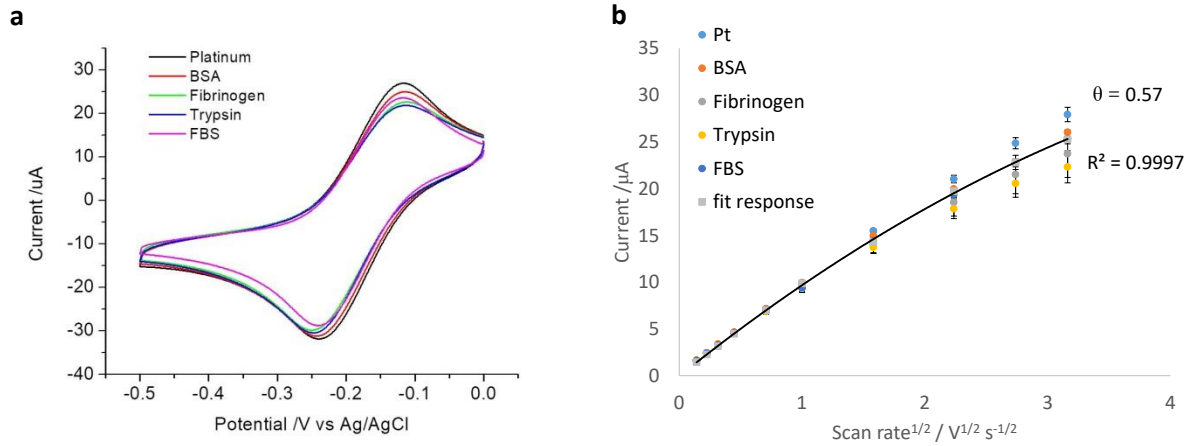

Figure 8